

Orbital Orders and Possible non-Fermi Liquid in Moiré systems

Yichen Xu,¹ Xiao-Chuan Wu,¹ Chao-Ming Jian,² and Cenke Xu¹

¹*Department of Physics, University of California, Santa Barbara, CA 93106, USA*

²*Station Q, Microsoft, Santa Barbara, California 93106-6105, USA*

Motivated by recent observation of nematicity in Moiré systems, we study three different orbital orders that potentially can happen in Moiré systems: (1) the nematic order; (2) the valley polarization; and (3) the “compass order”. Each order parameter spontaneously breaks part of the spatial symmetries of the system. We explore physics caused by the quantum fluctuations close to the order-disorder transition of these order parameters. Especially, we recognize that the symmetry of the Moiré systems leads to a crucial difference of the effective theory describing the nematic order from the standard Hertz-Millis formalism. We demonstrate that this key difference may lead to a special non-Fermi liquid behavior near the order-disorder nematic transition, different from the standard non-Fermi liquid behavior usually expected when a Fermi surface is coupled to the critical fluctuations of orbital orders. We also discuss the interplay of the three order parameters and the possible rich phase diagram at finite temperature. Within the three orbital orders, the valley polarization and the “compass order” likely strongly compete with the superconductor.

PACS numbers:

I. INTRODUCTION

Systems with Moiré superlattice have surprised the condensed matter community with a plethora of correlated phenomena, supposedly due to the strong Coulomb interaction and the narrowness of the minibands in the Moiré mini Brillouin zone^{1–7}. Correlated insulator at fractional fillings^{8,9}, high temperature superconductor (compared with the miniband width)^{5–7,10–15}, quantum anomalous Hall effect^{16–19}, strange metal (non-Fermi liquid)^{20,21}, competing orders^{22,23}, spin-triplet pairing^{5–7,24} have all been reported in recent experiments on Moiré systems. Many of these phenomena may have to do with order parameters with nontrivial transformations under spatial symmetries, *i.e.* the orbital orders. For example, the quantum anomalous Hall effect definitely requires valley polarization because the Chern numbers of two degenerate minibands from two different valleys must cancel each other due to symmetry^{16–19}. Also, strong signature of nematic anisotropy was found in recent experiments on twisted bilayer graphene, in both the superconductor phase and the metallic phase^{22,23}. Mean field analysis of orbital orders in lattice models related to Moiré systems have also been studied²⁵.

Motivated by the experimental observations, in this work we discuss possible orbital orders in Moiré systems. We will explore novel generic physics at the order-disorder transition of the orbital orders, based on the spatial symmetries of the systems. Three different kinds of orbital orders, *i.e.* (1) the nematic order, (2) valley polarization, and (3) “compass order”, which spontaneously break different subgroups of the entire spatial symmetries will be discussed. These orders should be viewed as possible instability of Fermi surface due to interactions. We will focus on the order-disorder quantum phase transition of these order parameters, and especially how the quantum fluctuations of these order parameters may affect the electrons. We demonstrate that, due to the unique sym-

metry of the systems, the nematic order fluctuation may lead to a special non-Fermi liquid behavior, different from what is usually expected at the quantum critical regime of an orbital order. The interplay between these order parameters allows a very rich phase diagram at zero and finite temperature. Within these three orbital orders, the valley polarization and “compass order” can potentially strongly compete with the superconductor.

II. THREE ORBITAL ORDERS

In all the Moiré systems discovered so far, the most general microscopic symmetry is $C_3 \times \mathcal{T}$, where \mathcal{T} is an effective time-reversal symmetry which is a product between the ordinary time-reversal and a spin-flipping, hence this effective time-reversal symmetry still holds even with a background Zeeman field (inplane magnetic field). Under this symmetry, the Fermi surface of the miniband emerging from each valley only has a C_3 symmetry, and \mathcal{T} interchanges the two valleys. The dispersion of the minibands from the two valleys satisfy $\varepsilon_1(\vec{k}) = \varepsilon_2(-\vec{k})$, where the subscript is the valley index. Different Moiré systems have different extra symmetries, for example the twisted bilayer graphene (TBG) without alignment with the BN substrate has an inversion symmetry \mathcal{I} , while the trilayer graphene and h-BN heterostructure has a reflection symmetry \mathcal{P} ²⁶. Both \mathcal{I} and \mathcal{P} interchange the two valleys^{26–28}. We assume that the system under study has the symmetry $C_3 \times \mathcal{T} \times \mathcal{I}$. Under these spatial symmetries, the momenta and electron operators transform as

$$\begin{aligned} C_3 &: (k_x + ik_y) \rightarrow e^{i2\pi/3}(k_x + ik_y); \\ \mathcal{T} &: c_{a,\vec{k}} \rightarrow \tau_{ab}^1 c_{b,-\vec{k}}, \quad \mathcal{I} : c_{a,\vec{k}} \rightarrow \tau_{ab}^1 c_{b,-\vec{k}}, \end{aligned} \quad (1)$$

where a, b are the valley indices. In this work we will discuss three different orbital orders, each breaking different

subgroups of the entire symmetry $C_3 \times \mathcal{T} \times \mathcal{I}$.

The first orbital order we will consider is the nematic order ϕ , which is a complex scalar order parameter. The microscopic operator of the nematic order parameter in a two dimensional ($2d$) rotational invariant system can be written as²⁹

$$\hat{\phi}(\vec{x}) \sim \psi^\dagger(\vec{x})(\partial_x^2 - \partial_y^2 + i2\partial_x\partial_y)\psi(\vec{x}), \quad (2)$$

where $\psi(x)$ is the real space electron operator. $\hat{\phi}$ is an operator with zero or small momentum compared with the Fermi wave vector. In a system with symmetry $C_3 \times \mathcal{T} \times \mathcal{I}$, the zero momentum nematic operator can be represented as

$$\begin{aligned} \hat{\phi} \sim & \sum_{\vec{k}} c_{1,\vec{k}}^\dagger (k_x^2 - k_y^2 + 2ik_xk_y + \alpha(k_x - ik_y)) c_{1,\vec{k}} \\ & + \sum_{\vec{k}} c_{2,\vec{k}}^\dagger (k_x^2 - k_y^2 + 2ik_xk_y - \alpha(k_x - ik_y)) c_{2,\vec{k}} \end{aligned} \quad (3)$$

with real number α . Since the Fermi surface on each valley only has a C_3 symmetry, the $d_{x^2-y^2} + id_{xy}$ order parameter with angular momentum (+2) will mix with a $p_x - ip_y$ order parameter with angular momentum (-1). The nematic order parameter $\phi \sim \langle \hat{\phi} \rangle$ transforms under the symmetries as

$$C_3 : \phi \rightarrow e^{i2\pi/3}\phi; \quad \mathcal{T} : \phi \rightarrow \phi^*, \quad \mathcal{I} : \phi \rightarrow \phi. \quad (4)$$

A nonzero condensate of ϕ will break the spatial symmetries down to \mathcal{T} and \mathcal{I} only, and in this sense we can still refer to ϕ as a nematic order parameter. Nematic order has been found in many condensed matter systems (for a review see Ref. 30), and strong signature of the existence of nematic order in both the superconducting phase and the normal metallic phase was recently reported in TBG^{22,23}.

The second orbital order we will discuss is the valley polarization Φ , which corresponds to an operator

$$\hat{\Phi} \sim \sum_{\vec{k}} c_{1,\vec{k}}^\dagger c_{1,\vec{k}} - c_{2,\vec{k}}^\dagger c_{2,\vec{k}}. \quad (5)$$

A valley polarization $\Phi \sim \langle \hat{\Phi} \rangle$ is an Ising like order parameter. A nonzero Φ will cause imbalance of the electron density between the two valleys, *i.e.* the electron has higher population at one valley than the other, and it may lead to the quantum anomalous Hall effect¹⁶⁻¹⁹. Φ preserves the C_3 symmetry, but breaks both \mathcal{T} and \mathcal{I} .

The last order parameter is the “compass order” which is again a complex scalar order parameter. The microscopic compass order operator is represented as

$$\begin{aligned} \hat{\phi} \sim & \sum_{\vec{k}} c_{1,\vec{k}}^\dagger (k_x^2 - k_y^2 + 2ik_xk_y + \alpha(k_x - ik_y)) c_{1,\vec{k}} \\ & - \sum_{\vec{k}} c_{2,\vec{k}}^\dagger (k_x^2 - k_y^2 + 2ik_xk_y - \alpha(k_x - ik_y)) c_{2,\vec{k}} \end{aligned} \quad (6)$$

Under the symmetry actions, the compass order parameter $\varphi \sim \langle \hat{\phi} \rangle$ transforms as

$$C_3 : \varphi \rightarrow e^{i2\pi/3}\varphi; \quad \mathcal{T} : \varphi \rightarrow -\varphi^*, \quad \mathcal{I} : \varphi \rightarrow -\varphi. \quad (7)$$

The symmetry transformation of φ can be viewed as the definition of the order parameter. φ also has the same symmetry transformation as the composite field $\phi\Phi$.

The full symmetry $C_3 \times \mathcal{T} \times \mathcal{I}$ guarantees that, a nonzero nematic order leads to three different degenerate ground states, while a compass order can take six different expectation values with degenerate energy. The compass order and valley polarization both break time-reversal symmetry \mathcal{T} , hence both orders can lead to anomalous Hall effect, as was observed in Ref. 18,19. Since the nematic order preserves \mathcal{T} , a nematic order alone cannot lead to the anomalous Hall signal. But a nematic order breaks the rotation symmetry, hence it directly couples to the background strain of the system.

III. ORDER-DISORDER TRANSITION OF THE NEMATIC ORDER

Normally when an order parameter with zero or small momentum couples to the Fermi surface, the dynamics of the order parameter is over-damped at low frequency according to the standard Hertz-Millis theory^{31,32}. The nematic order parameter is slightly more complicated, when coupled to a circular Fermi surface, the dynamics of the nematic order parameter is decomposed into a transverse mode and longitudinal mode, and only the longitudinal mode is over-damped. The separation of the two modes was computed explicitly in Ref. 29, whose physical picture can be understood as following. Consider a general order parameter with a small momentum \vec{q} , the over-damping of this mode comes from its coupling with the patch of Fermi surface where the tangential direction is parallel with \vec{q} . For a circular Fermi surface, without loss of generality, let us assume $\vec{q} = (q_x, 0)$, then the Fermi patches that cause over-damping locate at $\vec{k}_f \sim \pm\hat{y}$. But $\text{Im}[\phi]$ defined previously has nodes along the $\pm\hat{y}$ direction (rotational invariance guarantees that the “tangential patch” of the Fermi surface coincides with the node of the transverse mode), hence $\text{Im}[\phi]_{\vec{q}}$ with $\vec{q} = (q_x, 0)$ is not over-damped.

But now the symmetry of the system, especially the fact that the d -wave order parameter mixes with the p -wave order parameter, no longer guarantees that for any small momentum \vec{q} the “tangential patch” of the Fermi surface coincides with the node of the order parameter, hence ϕ is always over-damped, which can be shown with explicit calculations following Ref. 29. Thus we will start with the following Hertz-Millis type of action for the nematic order parameter ϕ , which is invariant under the symmetry $C_3 \times \mathcal{T} \times \mathcal{I}$:

$$S_b = S_0 + \int d^2x d\tau u(\phi^3 + \phi^{*3}) + g|\phi|^4,$$

$$\mathcal{S}_0 = \sum_{\vec{q}, \omega} \phi_{\vec{q}, \omega}^* \left(\frac{|\omega|}{q} + q^2 + r \right) \phi_{\vec{q}, \omega} \quad (8)$$

For convenience we have written the free part of the action \mathcal{S}_0 in the momentum and Matsubara frequency space, but the interaction terms of the action in the Euclidean space-time. Also, since the U(1) rotation of ϕ is in fact a spatial rotation, there should be coupling between the direction of $\vec{\phi} = (\text{Re}[\phi], \text{Im}[\phi])$ and direction of momentum, which we have ignored for simplicity⁵⁵. Following the standard Hertz-Millis theory^{31,32}, the action Eq. 8 is scaling invariant if we assign the following scaling dimensions to the parameters and field:

$$[\omega] = 3, \quad [q_x] = [q_y] = 1, \quad [r] = 2, \\ [\phi(\vec{x}, \tau)] = \frac{3}{2}, \quad [u] = \frac{1}{2}, \quad [g] = -1. \quad (9)$$

At the level of the Hertz-Millis theory, normally the total space-time dimension is greater than the upper critical dimension, hence the self-interaction of the order parameter is usually irrelevant, and the theory will lead to an ordinary mean field transition (for a review see Ref. 33). However, unlike the ordinary Hertz-Millis theory, in our current case there is an extra symmetry-allowed term $u(\phi^3 + \phi^{*3})$ that is relevant even though the total space-time dimension is $D = d + z = 5$. Thus we need to perform analysis beyond the mean field theory, and explore the possible new physics led by the new term.

The relevant u term breaks the U(1) symmetry of ϕ down to a Z_3 symmetry, which is the symmetry of a three-state clock model³⁴. A mean field analysis of such Ginzburg-Landau theory would lead to a first order transition which occurs at $r_c = u^2/g$, but a two dimensional three-state clock model (equivalent to a three-state Potts model) has a continuous transition and can be potentially described by the Ginzburg-Landau theory with a Z_3 anisotropy on a U(1) order parameter³⁵. Ref. 36,37 also presented examples of first order quantum phase transitions at the mean field level (precisely due to a cubic term like our u -term in the action) being driven to continuous transitions by fluctuations, especially when the order parameter is coupled to gapless fermions³⁷, which is analogous to our situation.

Without knowing for sure the true nature of the transition described by Eq. 8, at least the scaling analysis in the previous paragraph applies when r is tuned *close to* while *greater than* r_c , and in the energy scale $\omega \gg (u^2/g)^{3/2}$ the order parameter ϕ can always be viewed as a massless scalar field with self-interaction u and g in Eq. 8.

If we further assume that $(u^2/g)^{3/2} \ll 1/g^3$ and only look at energy scale $\omega < 1/g^3$, the irrelevant coupling g is renormalized small enough. Hence when the parameters in Eq. 8 satisfy $(u^2/g)^{3/2} \ll 1/g^3$, there is a finite energy window $\omega \in ((u^2/g)^{3/2}, 1/g^3)$ where we can view ϕ as a massless scalar field which interacts with itself mainly through the u term in Eq. 8, and the ordinary

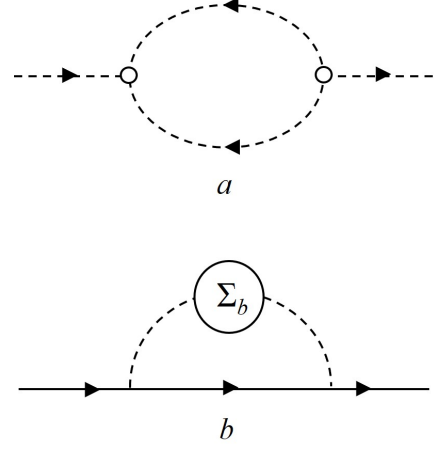


FIG. 1: *a*, the one-loop correction to the boson propagator from the u term in Eq. 8; *b*, the one-loop correction (Eq. 14) to the fermion propagator through the boson-fermion coupling g' in Eq. 12.

$|\phi|^4$ interaction is irrelevant and renormalized perturbatively weak. We expect that the action Eq. 8 with the relevant interaction u can lead to new universal physics that is beyond the standard Hertz-Millis theory.

Based on Eq. 8, if we take into account of the relevant perturbation u , in general the boson propagator reads

$$G_b(\omega, \vec{q}) = \frac{1}{G_{b0}^{-1}(\omega, \vec{q}) + \Sigma_b(\omega, \vec{q})}, \\ G_{b0}^{-1}(\omega, \vec{q}) = \frac{|\omega|}{q} + q^2. \quad (10)$$

A full reliable analysis of Eq. 8 with the relevant perturbation u is difficult, we will first limit our study to the lowest nontrivial order of perturbation of u , later we will discuss other analysis. At the one-loop level (Fig. 1*a*), the boson self-energy $\Sigma_b(\omega, \vec{p})$ reads

$$\Sigma_b(\omega, \vec{q}) \sim u^2 \int d^2 k d\nu G_{b0}(\nu, \vec{k}) G_{b0}(\omega + \nu, \vec{q} + \vec{k}), \\ \sim \text{Const} + Au^2 \sqrt{|\omega|^{2/3} + cq^2} + \dots \quad (11)$$

A and c are both order one constants. The behavior of the boson self-energy is consistent with power-counting of the loop integral, and at low energy it dominates other quadratic terms \mathcal{S}_0 in the standard Hertz-Millis theory, due to the fact that u is a relevant perturbation. The cut-off dependent constant can be reabsorbed into r , and the ellipsis includes terms that are less dominant in the infrared⁵⁶.

For our purpose we need to analyze the effects of the boson-fermion coupling on the electrons. In the standard Hertz-Millis theory without the relevant u term in the boson action, the one loop self-energy of the electron scales as $\Sigma_f(\omega) \sim \text{sgn}[\omega]|\omega|^{2/3}$. We will analyze how the u term may change the behavior of the fermion self-energy.

Following the formalism used in Ref. 38–42, we expand the system at one patch of the Fermi surface. The “one-patch” theory is a very helpful formalism to systematically evaluate loop diagrams in a boson-fermion coupled theory. This “one-patch theory” breaks the C_3 symmetry, hence the real and imaginary parts of ϕ are no longer degenerate. Since we are most interested in the scaling behavior of the Fermion self-energy, we will consider a one component boson field with the dressed propagator and self-energy given by Eq. 11. The one-patch theory reads

$$\begin{aligned} \mathcal{S}_{bf} = & \sum_{\omega, \vec{k}} \psi_{\omega, \vec{k}}^\dagger (i\omega - v_f k_x - v k_y^2) \psi_{\omega, \vec{k}} \\ & + \mathcal{S}_0 + \sum_{\omega, \vec{q}} \Sigma_b(\omega, \vec{q}) |\phi_{\omega, \vec{q}}|^2 \\ & + \int d^2x d\tau g' \phi \psi^\dagger \psi, \end{aligned} \quad (12)$$

Where \mathcal{S}_0 is given by Eq. 8, and $\Sigma_b(\omega, \vec{q})$ given by Eq. 11.

For this “one-patch” boson-fermion coupled theory we need to use a different assignment of scaling dimensions, which was introduced in Ref. 38–42 for a better controlled analysis of the boson-fermion coupled theory. In order to avoid confusion, we use “[]” to denote the scaling dimension of the original pure boson theory Eq. 8, but “{ }” to denote the scaling dimension of the “one-patch” boson-fermion coupled theory:

$$\begin{aligned} \{\omega\} = 3, \quad \{k_x\} = 2, \quad \{k_y\} = 1, \\ \{\phi(\vec{x}, \tau)\} = \frac{5}{2}, \quad \{\psi\} = 2, \quad \{g'\} = -\frac{1}{2}. \end{aligned} \quad (13)$$

Under the new scaling relation Eq. 13, \mathcal{S}_0 becomes irrelevant compared with $\Sigma_b(\omega, \vec{q})$ in Eq. 11. We will first ignore the irrelevant term \mathcal{S}_0 completely (which will be revisited later) to reveal the main effect of the new u -term in Eq. 8. The one-loop fermion self-energy (Fig. 1b) reads

$$\begin{aligned} \Sigma_f(\omega) & \sim \int d^2k d\nu G_{f0}(\nu, \vec{k}) G_b(\omega + \nu, \vec{k}) \\ & \sim \int d^2k d\nu \frac{1}{i\nu - v_f k_x - v k_y^2} \frac{1}{\sqrt{|\omega + \nu|^{2/3} + c k^2}} \\ & \sim i\omega \log\left(\frac{\Lambda}{|\omega|}\right). \end{aligned} \quad (14)$$

This behavior of fermion self-energy is similar to the marginal fermi liquid, and it is consistent with the simple power-counting of the loop integral. The marginal fermi liquid was proposed as a phenomenological theory for the strange metal phase (a non-Fermi liquid phase) of the cuprates high temperature superconductor⁴³. A similar strange metal behavior was observed in the TBG^{20–22}. Our goal here is not to directly address the observed strange metal behavior⁵⁷, instead we stress that the electrons at the order-disorder transition of the nematic order in the Moiré systems should behave differently from what is usually expected at a nematic quantum critical point.

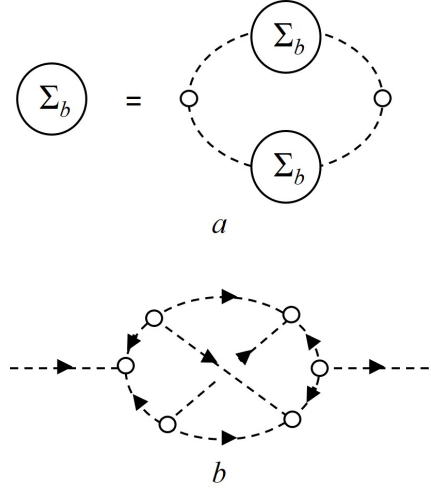


FIG. 2: *a*, the schematic representation of the Schwinger-Dyson equation; *b*, the example of vertex correction that is not summed in the Schwinger-Dyson equation.

This difference originates from the unique symmetry of the Moiré systems.

Because g' is an irrelevant perturbation in Eq. 12 according to the scaling convention of the “one-patch” theory Eq. 13, higher order perturbation of g' in theory Eq. 12 is not expected to lead to more dominant correction to the fermion self-energy in the infrared, hence we no longer need to worry about the infinite “planar diagram” problem in ordinary cases when an order parameter is coupled with a Fermi surface⁴¹.

The results above are based on the one-loop calculation in the expansion of u , and higher order expansion of u will modify the results in the infrared limit. If eventually the nematic transition is driven continuous by fluctuations as the examples given in Ref. 36,37, then a full analysis for the infrared limit is desired. Although we cannot completely solve the strongly interacting theory Eq. 8 analytically beyond the perturbation expansion, an approximate solution can be obtained through the Schwinger-Dyson (SD) equation, which sums a subset of the Feynman diagrams Fig. 2a:

$$\begin{aligned} \Sigma_b & \sim u^2 \int d^2k d\nu G_b(\nu, \vec{k}) G_b(\omega + \nu, \vec{q} + \vec{k}), \\ G_b^{-1} & = G_{b0}^{-1} + \Sigma_b. \end{aligned} \quad (15)$$

Here we have ignored the vertex correction from the full SD equation (For example, vertex correction Fig. 2b). We also take a simple ansatz that at the order-disorder transition the boson self-energy is approximated by the scaling form

$$\Sigma_b(\omega, \vec{q}) \sim u^{2\eta} Q^{2-\eta} \quad (16)$$

with anomalous dimension η , where Q is the infrared cut-off that can be taken as $\text{Max}[|\omega|^{1/3}, |\vec{q}|]$. The previous one-loop result simply yields $\eta = 1$. Now the bosonic

part of the boson-fermion coupling action Eq. 12 is replaced by $\mathcal{S}_b = \mathcal{S}_0 + \sum_{\omega, \vec{q}} \Sigma_b(\omega, \vec{q}) |\phi_{\omega, \vec{q}}|^2$. Again, if we tentatively ignore \mathcal{S}_0 , the scaling of the boson-fermion coupling theory is modified as

$$\{\omega\} = 3, \quad \{k_x\} = 2, \quad \{k_y\} = 1, \\ \{\phi(\vec{x}, \tau)\} = \frac{4+\eta}{2}, \quad \{\psi\} = 2, \quad \{g'\} = -\frac{\eta}{2}. \quad (17)$$

The one-loop fermion self-energy should then scale as

$$\Sigma_f(\omega) \sim i\omega|\omega|^{\frac{\eta-1}{3}}. \quad (18)$$

As long as $\eta > 0$, the boson-fermion coupling g' in Eq. 12 is still irrelevant, hence higher order fermion self-energy diagrams from the boson-fermion coupling theory are not expected to change Eq. 18 in the infrared.

The solution of the approximate SD equation would yield $\eta = 1/3$, which will lead to a non-fermi liquid behavior that is in-between the standard Hertz-Millis theory and also the marginal fermi liquid. After we convert the Matsubara frequency to real frequency, the imaginary part of the fermion self-energy (inverse of the fermion life-time) is a very characteristic property of the non-Fermi liquid. And the analysis above suggests that the imaginary part of fermion self-energy should scale as $\text{Im}(\Sigma_f) \sim \text{sgn}(\omega)|\omega|^\beta$ with $2/3 < \beta < 1$.

If eventually the transition in Eq. 8 is driven continuously by fluctuation (like the examples given in Ref. 36,37), then the field ϕ is indeed massless even in the infrared limit at the transition. Then the difference of our results described above from the standard Hertz-Millis theory should be obvious in the infrared limit. But even if the transition is first order at $r_c = u^2/g$, as we discussed previously, when the parameters in Eq. 8 satisfy $(u^2/g)^{3/2} \ll 1/g^3$, at least there is a finite energy window $|\omega| \in ((u^2/g)^{3/2}, 1/g^3)$ where ϕ can be viewed as a massless scalar field with strong self-interaction mainly through the u term, while other interactions in Eq. 8 can be ignored. In this case, the calculations in this section were simplified by assuming that the boson self-energy Σ_b dominates the other quadratic term, *i.e.* \mathcal{S}_0 in Eq. 8, because \mathcal{S}_0 is irrelevant compared with Σ_b . But in the finite energy window described above, since we are not in the infrared limit, one should keep a nonzero \mathcal{S}_0 together with Σ_b in the calculation of the fermion self-energy. Then the loop integral in the evaluation of $\Sigma_f(\omega)$ is more complicated. The fermion self-energy is no longer a simple scaling form $\text{Im}(\Sigma_f) \sim \text{sgn}(\omega)|\omega|^\beta$ with a constant exponent β . Instead, the exponent β is expected to increase from the standard Hertz-Millis result $\beta = 2/3$ while decreasing ω , *i.e.* in other words the system should crossover back to the standard Hertz-Millis result at higher energy scale. We have numerically calculated the fermion self-energy by keeping a nonzero \mathcal{S}_0 in the bosonic theory, and confirmed this expectation of crossover.

Recently the standard result of the fermion self-energy scaling of the Hertz-Millis theory was confirmed in numerical simulation⁴⁴ on nematic transitions on a square

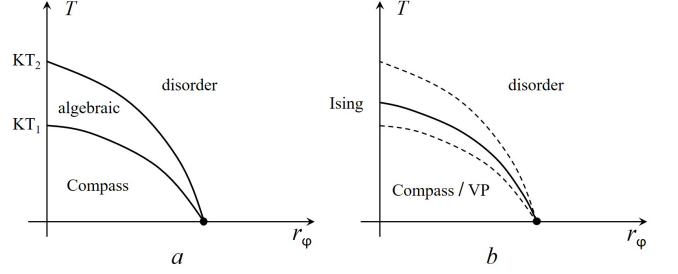


FIG. 3: *a*, the phase diagram when there is a compass order at zero temperature, there are two consecutive Kosterlitz-Thouless transitions at finite temperatures and an algebraic phase in between; *b*, once there is a background strain in the system, the compass order is identical to the valley polarization (VP) order, and hence there is only one Ising transition at finite temperature.

lattice. We expect that our qualitative prediction of the fermion self-energy under the symmetry of the Moiré systems can also be seen in future numerical simulations.

IV. VALLEY POLARIZATION AND COMPASS ORDER

The effective theory of the valley polarization order Φ and compass order φ are more conventional Hertz-Millis theories whose analysis can be quoted from Ref. 33. A cubic self-interaction term is not allowed for either order parameters. But the symmetry transformation of the compass order φ allows a term

$$u_6(\varphi^6 + \varphi^{*6}) \quad (19)$$

in the Ginzburg-Landau-Hertz-Millis theory of φ , which is irrelevant in the infrared at the total space-time dimension $D = 5$. The three order parameters are coupled together in the effective theory, and the lowest order symmetry-allowed couplings are:

$$\begin{aligned} \mathcal{L}_{mix} = & \dots + r_\phi |\phi|^2 + r_\varphi |\varphi|^2 + r_\Phi |\Phi|^2 \\ & + v_1(\Phi\phi\varphi^* + h.c.) + v_2(\Phi\varphi^3 + h.c.) \\ & + v_3\Phi^2|\phi|^2 + v_4\Phi^2|\varphi|^2. \end{aligned} \quad (20)$$

A full exploration of the multi-dimensional parameter space will lead to a very complex and rich phase diagram. The specific values of the parameters in Eq. 20 depend heavily on the microscopic physics of the system.

Recently evidence of strain that breaks the C_3 rotation symmetry has been reported in Moiré systems⁴⁵, and the strain can potentially strongly affect the band structure⁴⁶. With a background strain field, the nematic order parameter ϕ acquires a nonzero expectation value, and hence Φ and φ become the same order parameter through the coupling v_1 in \mathcal{L}_{mix} .

At finite temperature, the nematic order and valley polarization will go through continuous transitions which correspond to the three-state Potts and Ising conformal field theory with central charges $4/5$ and $1/2$ respectively. While if we start with a zero temperature compass order, the finite temperature physics can be mapped to a six-state clock model due to the u_6 term mentioned previously in the Ginzburg-Landau theory of the compass order. In this case while raising temperature the system will undergo two consecutive continuous Kosterlitz-Thouless transitions with an algebraic quasi-long range order in between. Within the algebraic phase, the scaling dimension of the compass order parameter $[\varphi]$ is temperature dependent, and $1/18 < [\varphi] < 1/8$. The nematic order parameter $\phi \sim \varphi^2$ and valley polarization $\Phi \sim \varphi^3 + \varphi^{*3}$ also have power-law correlation function in the algebraic phase, and their scaling dimensions are $[\phi] = 4[\varphi]$, and $[\Phi] = 9[\varphi]$. Hence even a weak background strain which pins ϕ is always a relevant perturbation in the algebraic phase, and will collapse the two Kosterlitz-Thouless transitions of φ into a single Ising transition of Φ .

Signature of a hidden order which strongly competes with superconductor was observed experimentally^{22,23}. Within the three orbital orders that we have discussed in this work, the valley polarization and compass order both obviously compete with the superconductor. The reason is that both these two order parameters break \mathcal{T} and \mathcal{I} , hence break the degeneracy between electrons at \vec{k} and $-\vec{k}$ (the C_3 symmetry alone does not protect this degeneracy), hence a nonzero Φ or φ makes it difficult to form zero momentum Cooper pair. Indeed, experiments so far have not found superconductivity near the quantum anomalous Hall state in Moiré systems which at least require either valley polarization or the compass order. We stress that the competing order mentioned here does not necessarily mean it is the nature of the correlated insulator observed experimentally.

V. FINAL REMARKS

In this work we studied three different orbital orders that may occur in Moiré systems. We demonstrate that

at the order-disorder transition of the nematic order parameter (one of the three orbital orders), a special non-Fermi liquid behavior is expected in a finite energy window, due to the symmetry of the system. We focused on the metallic phase at the disorder-order transition of the orbital order, since experimentally a nematic metallic phase was observed²³ above the nematic superconducting phase. Since the three different orbital orders can interact with each other in the effective theory and lead to a complex and rich phase diagram, depending on the parameters the Moiré systems under different conditions may display different orbital orders. We demonstrate that the effective theory for the nematic order is beyond the standard Hertz-Millis theory. Numerical methods such as Ref. 44,47–49 are demanded to verify the results in the current work.

We focused on the generic field theory analysis of the phase transitions of the orbital orders, based on the symmetry of the system. The parameters of the field theory can be estimated through a calculation based on the lattice models, but this estimate depends on the microscopic details of the systems, and it may vary strongly between different systems. For example, the parameter u stems from the C_3 symmetry of the Fermi surface at each valley, and its value depends on the extent of the C_3 deformation from the ordinary circular Fermi surface, which likely strongly depends on the microscopic model as well as the charge density. Due to the complexity and subtlety of the microscopic analysis, we plan to leave it to future studies. In the future we will also pursue a proper generalized renormalization group expansion such as Ref. 38–40, as well as analysis of the stability of the nematic order transition towards other orders such as superconductivity^{50–53} in Moiré systems.

The authors thank Leon Balents, Steve Kivelson for helpful discussions. This work is supported by NSF Grant No. DMR-1920434, the David and Lucile Packard Foundation, and the Simons Foundation.

-
- ¹ R. Bistritzer and A. H. MacDonald, Proceedings of the National Academy of Sciences **108**, 12233 (2011), ISSN 0027-8424, <http://www.pnas.org/content/108/30/12233.full.pdf>, URL <http://www.pnas.org/content/108/30/12233>.
 - ² E. Suárez Morell, J. D. Correa, P. Vargas, M. Pacheco, and Z. Barticevic, Phys. Rev. B **82**, 121407 (2010), URL <https://link.aps.org/doi/10.1103/PhysRevB.82.121407>.
 - ³ S. Fang and E. Kaxiras, Phys. Rev. B **93**, 235153 (2016), URL [https://link.aps.org/doi/10.1103/PhysRevB.](https://link.aps.org/doi/10.1103/PhysRevB.93.235153)

93.235153.

- ⁴ G. Trambly de Laissardière, D. Mayou, and L. Magaud, Phys. Rev. B **86**, 125413 (2012), URL <https://link.aps.org/doi/10.1103/PhysRevB.86.125413>.
- ⁵ C. Shen, Y. Chu, Q. Wu, N. Li, S. Wang, Y. Zhao, J. Tang, J. Liu, J. Tian, K. Watanabe, et al., Nature Physics (2020), ISSN 1745-2481, URL <http://dx.doi.org/10.1038/s41567-020-0825-9>.
- ⁶ X. Liu, Z. Hao, E. Khalaf, J. Y. Lee, K. Watanabe, T. Taniguchi, A. Vishwanath, and P. Kim (2019), 1903.08130.

- ⁷ Y. Cao, D. Rodan-Legrain, O. Rubies-Bigorda, J. M. Park, K. Watanabe, T. Taniguchi, and P. Jarillo-Herrero (2019), 1903.08596.
- ⁸ G. Chen, L. Jiang, S. Wu, B. Lyu, H. Li, B. L. Chittari, K. Watanabe, T. Taniguchi, Z. Shi, J. Jung, et al., *Nature Physics* **15**, 237C241 (2019), ISSN 1745-2481, URL <http://dx.doi.org/10.1038/s41567-018-0387-2>.
- ⁹ Y. Cao, V. Fatemi, A. Demir, S. Fang, S. L. Tomarken, J. Y. Luo, J. D. Sanchez-Yamagishi, K. Watanabe, T. Taniguchi, E. Kaxiras, et al., *Nature* **556**, 80 (2018).
- ¹⁰ Y. Cao, V. Fatemi, S. Fang, K. Watanabe, T. Taniguchi, E. Kaxiras, and P. Jarillo-Herrero, *Nature* **556**, 43 (2018).
- ¹¹ M. Yankowitz, S. Chen, H. Polshyn, Y. Zhang, K. Watanabe, T. Taniguchi, D. Graf, A. F. Young, and C. R. Dean, *Science* **363**, 1059 (2019), ISSN 0036-8075, <http://science.sciencemag.org/content/363/6431/1059.full.pdf>, URL <http://science.sciencemag.org/content/363/6431/1059>.
- ¹² G. Chen, A. L. Sharpe, P. Gallagher, I. T. Rosen, E. J. Fox, L. Jiang, B. Lyu, H. Li, K. Watanabe, T. Taniguchi, et al., *Nature* **572**, 215C219 (2019), ISSN 1476-4687, URL <http://dx.doi.org/10.1038/s41586-019-1393-y>.
- ¹³ A. L. Sharpe, E. J. Fox, A. W. Barnard, J. Finney, K. Watanabe, T. Taniguchi, M. A. Kastner, and D. Goldhaber-Gordon, *Science* **365**, 605C608 (2019), ISSN 1095-9203, URL <http://dx.doi.org/10.1126/science.aaw3780>.
- ¹⁴ P. Kim, *Ferromagnetic superconductivity in twisted double bilayer graphene*, http://online.kitp.ucsb.edu/online/bands_m19/kim/ (2019), Talks at KITP, Jan 15, 2019.
- ¹⁵ X. Lu, P. Stepanov, W. Yang, M. Xie, M. A. Aamir, I. Das, C. Urgell, K. Watanabe, T. Taniguchi, G. Zhang, et al., *Nature* **574**, 653C657 (2019), ISSN 1476-4687, URL <http://dx.doi.org/10.1038/s41586-019-1695-0>.
- ¹⁶ N. Bultinck, S. Chatterjee, and M. P. Zaletel, *Physical Review Letters* **124** (2020), ISSN 1079-7114, URL <http://dx.doi.org/10.1103/PhysRevLett.124.166601>.
- ¹⁷ Y.-H. Zhang, D. Mao, and T. Senthil, *Physical Review Research* **1** (2019), ISSN 2643-1564, URL <http://dx.doi.org/10.1103/PhysRevResearch.1.033126>.
- ¹⁸ G. Chen, A. L. Sharpe, E. J. Fox, Y.-H. Zhang, S. Wang, L. Jiang, B. Lyu, H. Li, K. Watanabe, T. Taniguchi, et al., *Nature* **579**, 56C61 (2020), ISSN 1476-4687, URL <http://dx.doi.org/10.1038/s41586-020-2049-7>.
- ¹⁹ M. Serlin, C. L. Tschirhart, H. Polshyn, Y. Zhang, J. Zhu, K. Watanabe, T. Taniguchi, L. Balents, and A. F. Young, *Science* **367**, 900C903 (2019), ISSN 1095-9203, URL <http://dx.doi.org/10.1126/science.aay5533>.
- ²⁰ Y. Cao, D. Chowdhury, D. Rodan-Legrain, O. Rubies-Bigorda, K. Watanabe, T. Taniguchi, T. Senthil, and P. Jarillo-Herrero, *Physical Review Letters* **124** (2020), ISSN 1079-7114, URL <http://dx.doi.org/10.1103/PhysRevLett.124.076801>.
- ²¹ H. Polshyn, M. Yankowitz, S. Chen, Y. Zhang, K. Watanabe, T. Taniguchi, C. R. Dean, and A. F. Young, *Nature Physics* **15**, 1011C1016 (2019), ISSN 1745-2481, URL <http://dx.doi.org/10.1038/s41567-019-0596-3>.
- ²² P. Jarillo-Herrero, *Magic Angle Graphene Transport Phenomenology*, http://online.kitp.ucsb.edu/online/bands_m19/jarilloherrero/ (2019).
- ²³ Y. Cao, D. Rodan-Legrain, J. M. Park, F. Noah Yuan, K. Watanabe, T. Taniguchi, R. M. Fernandes, L. Fu, and P. Jarillo-Herrero, arXiv e-prints arXiv:2004.04148 (2020), 2004.04148.
- ²⁴ J. Y. Lee, E. Khalaf, S. Liu, X. Liu, Z. Hao, P. Kim, and A. Vishwanath, *Nature Communications* **10** (2019), ISSN 2041-1723, URL <http://dx.doi.org/10.1038/s41467-019-12981-1>.
- ²⁵ J. F. Dodaro, S. A. Kivelson, Y. Schattner, X. Q. Sun, and C. Wang, *Phys. Rev. B* **98**, 075154 (2018), URL <https://link.aps.org/doi/10.1103/PhysRevB.98.075154>.
- ²⁶ H. C. Po, L. Zou, A. Vishwanath, and T. Senthil, *Phys. Rev. X* **8**, 031089 (2018), URL <https://link.aps.org/doi/10.1103/PhysRevX.8.031089>.
- ²⁷ L. Zou, H. C. Po, A. Vishwanath, and T. Senthil, *Phys. Rev. B* **98**, 085435 (2018), URL <https://link.aps.org/doi/10.1103/PhysRevB.98.085435>.
- ²⁸ Y.-H. Zhang and T. Senthil, *Physical Review B* **99** (2019), ISSN 2469-9969, URL <http://dx.doi.org/10.1103/PhysRevB.99.205150>.
- ²⁹ V. Oganessyan, S. A. Kivelson, and E. Fradkin, *Phys. Rev. B* **64**, 195109 (2001), URL <https://link.aps.org/doi/10.1103/PhysRevB.64.195109>.
- ³⁰ E. Fradkin, S. A. Kivelson, M. J. Lawler, J. P. Eisenstein, and A. P. Mackenzie, *Annual Review of Condensed Matter Physics* **1**, 153 (2010), <https://doi.org/10.1146/annurev-conmatphys-070909-103925>, URL <https://doi.org/10.1146/annurev-conmatphys-070909-103925>.
- ³¹ J. A. Hertz, *Phys. Rev. B* **14**, 1165 (1976), URL <https://link.aps.org/doi/10.1103/PhysRevB.14.1165>.
- ³² A. J. Millis, *Phys. Rev. B* **48**, 7183 (1993), URL <https://link.aps.org/doi/10.1103/PhysRevB.48.7183>.
- ³³ H. v. Löhneysen, A. Rosch, M. Vojta, and P. Wölfle, *Rev. Mod. Phys.* **79**, 1015 (2007), URL <https://link.aps.org/doi/10.1103/RevModPhys.79.1015>.
- ³⁴ F. Y. Wu, *Rev. Mod. Phys.* **54**, 235 (1982), URL <https://link.aps.org/doi/10.1103/RevModPhys.54.235>.
- ³⁵ F. Fucito and G. Parisi, *J. Phys. A: Math. Gen.* **14**, L507 (1981).
- ³⁶ Z. Bi, E. Lake, and T. Senthil, *Physical Review Research* **2** (2020), ISSN 2643-1564, URL <http://dx.doi.org/10.1103/PhysRevResearch.2.023031>.
- ³⁷ Z.-X. Li, Y.-F. Jiang, S.-K. Jian, and H. Yao, *Nature Communications* **8** (2017), ISSN 2041-1723, URL <http://dx.doi.org/10.1038/s41467-017-00167-6>.
- ³⁸ C. Nayak and F. Wilczek, *Nuclear Physics B* **417**, 359 (1994), ISSN 0550-3213, URL <http://www.sciencedirect.com/science/article/pii/0550321394904774>.
- ³⁹ C. Nayak and F. Wilczek, *Nuclear Physics B* **430**, 534 (1994), ISSN 0550-3213, URL <http://www.sciencedirect.com/science/article/pii/0550321394901589>.
- ⁴⁰ D. F. Mross, J. McGreevy, H. Liu, and T. Senthil, *Phys. Rev. B* **82**, 045121 (2010), URL <https://link.aps.org/doi/10.1103/PhysRevB.82.045121>.
- ⁴¹ S.-S. Lee, *Phys. Rev. B* **80**, 165102 (2009), URL <https://link.aps.org/doi/10.1103/PhysRevB.80.165102>.
- ⁴² M. A. Metlitski and S. Sachdev, *Phys. Rev. B* **82**, 075127 (2010), URL <https://link.aps.org/doi/10.1103/PhysRevB.82.075127>.
- ⁴³ C. M. Varma, P. B. Littlewood, S. Schmitt-Rink, E. Abrahams, and A. E. Ruckenstein, *Phys. Rev. Lett.* **63**, 1996 (1989), URL <https://link.aps.org/doi/10.1103/PhysRevLett.63.1996>.
- ⁴⁴ X. Y. Xu, A. Klein, K. Sun, A. V. Chubukov, and Z. Y. Meng, arXiv e-prints arXiv:2003.11573 (2020), 2003.11573.

- ⁴⁵ Y. Xie, B. Lian, B. Jäck, X. Liu, C.-L. Chiu, K. Watanabe, T. Taniguchi, B. A. Bernevig, and A. Yazdani, *Nature* **572**, 101 (2019).
- ⁴⁶ Z. Bi, N. F. Q. Yuan, and L. Fu, *Phys. Rev. B* **100**, 035448 (2019), URL <https://link.aps.org/doi/10.1103/PhysRevB.100.035448>.
- ⁴⁷ Y. Schattner, S. Lederer, S. A. Kivelson, and E. Berg, *Phys. Rev. X* **6**, 031028 (2016), URL <https://link.aps.org/doi/10.1103/PhysRevX.6.031028>.
- ⁴⁸ S. Lederer, Y. Schattner, E. Berg, and S. A. Kivelson, *Proceedings of the National Academy of Sciences* **114**, 4905 (2017), ISSN 0027-8424, <https://www.pnas.org/content/114/19/4905.full.pdf>, URL <https://www.pnas.org/content/114/19/4905>.
- ⁴⁹ X. Y. Xu, Z. Hong Liu, G. Pan, Y. Qi, K. Sun, and Z. Y. Meng, *Journal of Physics: Condensed Matter* **31**, 463001 (2019), ISSN 1361-648X, URL <http://dx.doi.org/10.1088/1361-648X/ab3295>.
- ⁵⁰ M. A. Metlitski, D. F. Mross, S. Sachdev, and T. Senthil, *Phys. Rev. B* **91**, 115111 (2015), URL <https://link.aps.org/doi/10.1103/PhysRevB.91.115111>.
- ⁵¹ S. Lederer, Y. Schattner, E. Berg, and S. A. Kivelson, *Phys. Rev. Lett.* **114**, 097001 (2015), URL <https://link.aps.org/doi/10.1103/PhysRevLett.114.097001>.
- ⁵² J. Rech, C. Pépin, and A. V. Chubukov, *Phys. Rev. B* **74**, 195126 (2006), URL <https://link.aps.org/doi/10.1103/PhysRevB.74.195126>.
- ⁵³ A. V. Chubukov, C. Pépin, and J. Rech, *Phys. Rev. Lett.* **92**, 147003 (2004), URL <https://link.aps.org/doi/10.1103/PhysRevLett.92.147003>.
- ⁵⁴ F. Wu, E. Hwang, and S. Das Sarma, *Phys. Rev. B* **99**, 165112 (2019), URL <https://link.aps.org/doi/10.1103/PhysRevB.99.165112>.
- ⁵⁵ The simplest nonzero term of this type would be $\int d^2x d\tau \phi(\partial_x - i\partial_y)^2 \phi$, which has the same scaling as the rest of the quadratic terms, hence it is not expected to lead to more singular contribution to the physical quantities to be calculated.
- ⁵⁶ The loop integral is performed numerically, and it fits best with the expression in Eq. 11.
- ⁵⁷ It was suggested that a pure phonon-electron coupling can lead to a linear- T resistivity in Moiré systems^{21,54}, but it was argued in Ref. 20 that other mechanisms may be demanded to explain the observed data.